CHAPTER 4

Bivariable and Multivariable Analysis of EEG Signals

Rodrigo Quian Quiroga

The chapters thus far have described quantitative tools that can be used to extract information from single EEG channels. In this chapter we describe measures of synchronization between different EEG recordings sites. The concept of synchronization goes back to the observation of the interaction between two pendulum clocks by the Dutch physicist Christiaan Huygens in the seventeenth century. Since the times of Huygens, the phenomenon of synchronization has been largely studied, especially for the case of oscillatory systems [1].

Before getting into technical details of how to measure synchronization, we first consider why it is important to measure synchronization between EEG channels. There are several reasons. First, synchronization measures can let us assess the level of functional connectivity between two areas. It should be stressed that functional connectivity is not necessarily the same as anatomical connectivity, since anatomical connections between two areas may be active only in some particular situations—and the general interest in neuroscience is to find out which situations lead to these connectivity patterns. Second, synchronization may have clinical relevance for the identification of different brain states or pathological activities. In particular, it is well established that epilepsy involves an abnormal synchronization of brain areas [2]. Third, related to the issue of functional connectivity, synchronization measures may show communication between different brain areas. This may be important to establish how information is transmitted across the brain or to find out how neurons in different areas interact to give rise to full percepts and behavior. In particular, it has been argued that perception involves massive parallel processing of distant brain areas, and the binding of different features into a single percept is achieved through the interaction of these areas [3, 4].

Even if outside the scope of this book, it is worth mentioning that perhaps the most interesting use of synchronization measures in neuroscience is to study how neurons encode information. There are basically two views. On the one hand, neurons may transmit information through precise synchronous firing; on the other hand, the only relevant information of the neuronal firing may be the average firing rate. Note that rather than having two extreme opposite views, one can also consider coding schemes in between these two, because the firing rate coding is more similar to a temporal coding when small time windows are used [5].

As beautifully described by the late Francisco Varela [6], synchronization in the brain can occur at different scales. For example, the coordinated firing of a large population of neurons can elicit spike discharges like the ones seen in Figure 4.1(b, c). The sole presence of spikes in each of these signals—or oscillatory activity as in the case of the signal shown in Figure 4.1(a)—is evidence for correlated activity at a smaller scale: the synchronous firing of single neurons.

The recordings in Figure 4.1 are from two intracranial electrodes in the frontal right and left lobes of male adult WAG/Rij rats, a genetic model for human absence epilepsy [7]. Signals were referenced to an electrode placed at the cerebellum, they were then bandpass filtered between 1 and 100 Hz and digitized at 200 Hz. The length of each dataset is 5 seconds long, which corresponds to 1,000 data points. This was the largest length in which the signals containing spikes could be visually judged as stationary.

As we mentioned, spikes are a landmark of correlated activity and the question arises of whether these spikes are also correlated across both hemispheres. The first guess is to assume that bilateral spikes may be a sign of generalized synchronization. It was actually this observation done by a colleague that triggered a series of papers by the author of this chapter showing how misleading it could be to establish synchronization patterns without proper quantitative measures [8]. For example, if we are asked to rank the synchronization level of the three signals of Figure 4.1, it seems

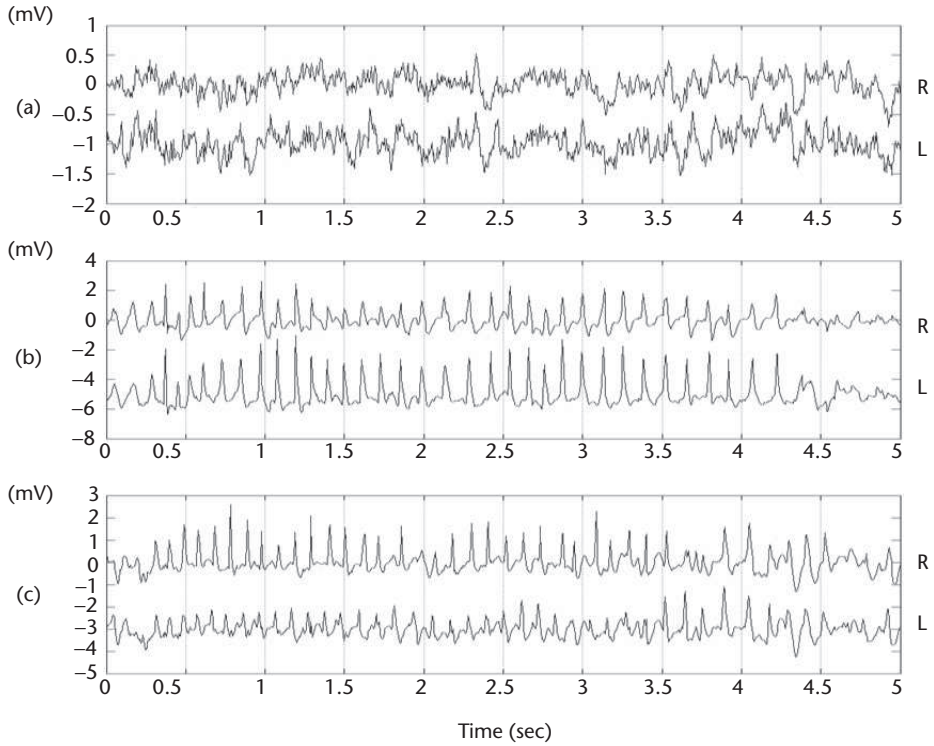

Figure 4.1 Three exemplary datasets of left and right cortical intracranial recordings in rats. (a) Normal looking EEG activity and (b, c) signals with bilateral spikes, a landmark of epileptic activity. Can you tell by visual inspection which of the examples has the largest and which one has the lowest synchronization across the left and right channels?

that the examples in Figure 4.1(b, c) should have the highest values, followed by the example of Figure 4.1(a). Wrong!

A closer look at Figure 4.1(c) shows that the spikes in both channels have a variable time lag. Just picking up the times of the maximum of the spikes in the left and right channels and calculating the lag between them, we determine that for Figure 4.1(b) the lag was very small and stable, between –5 and +5 ms—of the order of the sampling rate of these signals—and the standard deviation was of 4.7 ms [8]. In contrast, for Figure 4.1(c) the lag was much more variable and covered a range between –20 and 50 ms, with a standard deviation of 14.9. This clearly shows that in example B the simultaneous appearance of spikes is due to a generalized synchronization across hemispheres, whereas in Figure 4.1(c) the bilateral spikes are not synchronized and they reflect local independent generators for each hemisphere.

Interestingly, the signal of Figure 4.1(a) looks very noisy, but a closer look at both channels shows a strong covariance of these seemingly random fluctuations. Indeed, in a comprehensive study using several linear and nonlinear measures of synchronization, it was shown that the synchronization values are ranked as follows: $\text{Sync}_B > \text{Sync}_A > \text{Sync}_C$. This stresses the need for optimal measures to establish correlation patterns.

Throughout this chapter, we will use these three examples to illustrate the use of some of the correlation measures to be described. These examples can be downloaded from http://www.le.ac.uk/neuroengineering.

4.1 Cross-Correlation Function

The cross-correlation function is perhaps the most used measure of interdependence between signals in neuroscience. It has been, and continues to be, particularly popular for the analysis of similarities between spike trains of different neurons.

Let us suppose we have two simultaneously measured discrete time series x_n and y_n, $n = 1, \ldots, N$. The cross-correlation function is defined as

$$c_{xy}(\tau) = \frac{1}{N-\tau} \sum_{i=1}^{N-\tau} \left(\frac{x_i - \bar{x}}{\sigma_x} \right) \left(\frac{y_{i+\tau} - \bar{y}}{\sigma_y} \right) \tag{4.1}$$

where $\bar{x}$ and σ_x denote mean and variance and τ is the time lag. The cross-correlation function is basically the inner product between two normalized signals (that is, for each signal we subtract the mean and divide by the standard deviation) and it gives a measure of the linear synchronization between them as a function of the time lag τ. Its value ranges from –1, in the case of complete inverse correlation (that is, one of the signals is an exact copy of the other with opposite sign), to +1 for complete direct correlation. If the signals are not correlated, then the cross-correlation values will be around zero. Note, however, that noncorrelated signals will not give a value strictly equal to zero and the significance of nonzero cross-correlation values should be statistically validated, for example, using surrogate tests [9]. This basically implies generating signals with the same autocorrelation of the original ones but independent from each other. A relatively simple way of doing this is to shift one

of the signals with respect to the other and assume that they will not be correlated for large enough shifts [8].

Note that formally only the zero lag cross correlation can be considered to be a symmetric descriptor. Indeed, the time delay in the definition of (4.1) introduces an asymmetry that could, in principle, establish whether one of the signals leads or lags the other in time. It should be mentioned, however, that a time delay between two signals does not necessarily prove a certain driver-response causal relationship between them. In fact, time delays could be caused by a third signal driving both with a different delay or by internal delay loops of one of the signals [10].

Figure 4.2 shows the cross-correlation values for the three examples of Figure 4.1 as a function of the time delay τ. To visualize cross-correlation values with large time delays, we used here a slight variant of (4.1) by introducing periodic boundary conditions. The zero lag cross-correlation values are shown in Table 4.1. Here we see that the tendency is in agreement with what we expect from the arguments of the previous section; that is, $\text{Sync}_B > \text{Sync}_A > \text{Sync}_C$. However, the difference between examples A and B is relatively small. In principle, one expects that for long enough lags between the two signals the cross-correlation values should be close to zero. However, fluctuations for large delays are still quite large.

Taking these fluctuations as an estimation of the error of the cross-correlation values, one can infer that cross correlation cannot distinguish between the synchronization levels of examples A and B. This is mainly due to the fact that cross correlation is a linear measure and can poorly capture correlations between nonlinear signals, as is the case for examples B and C with the presence of spikes. More advanced nonlinear measures that are based on reconstruction of the signals in a phase space could indeed clearly distinguish between these two cases [8].

4.2 Coherence Estimation

The coherence function gives an estimation of the linear correlation between two signals as a function of the frequency. The main advantage over the cross-correlation function described in the previous section is that coherence is sensitive to interdependences that can be present in a limited frequency range. This is particularly interesting in neuroscience to establish how frequency bands may interact in different areas.

Let us first define the sample cross spectrum as the Fourier transform of the cross-correlation function, or by using the Fourier convolution theorem, as

$$C_{xy}(\omega) = (Fx)(\omega)\,(Fy)^{*}(\omega) \tag{4.2}$$

where (Fx) is the Fourier transform of x, ω are the discrete frequencies ($-N/2 < \omega < N/2$), and the asterisk indicates complex conjugation. The cross spectrum can be estimated, for example, using the Welch method [11]. For this, the data is divided into M epochs of equal length, and the spectrum of the signal is estimated as the average spectrum of these M segments. The estimated cross spectrum $\langle C_{xy}(\omega) \rangle$ is a complex number, whose normalized amplitude

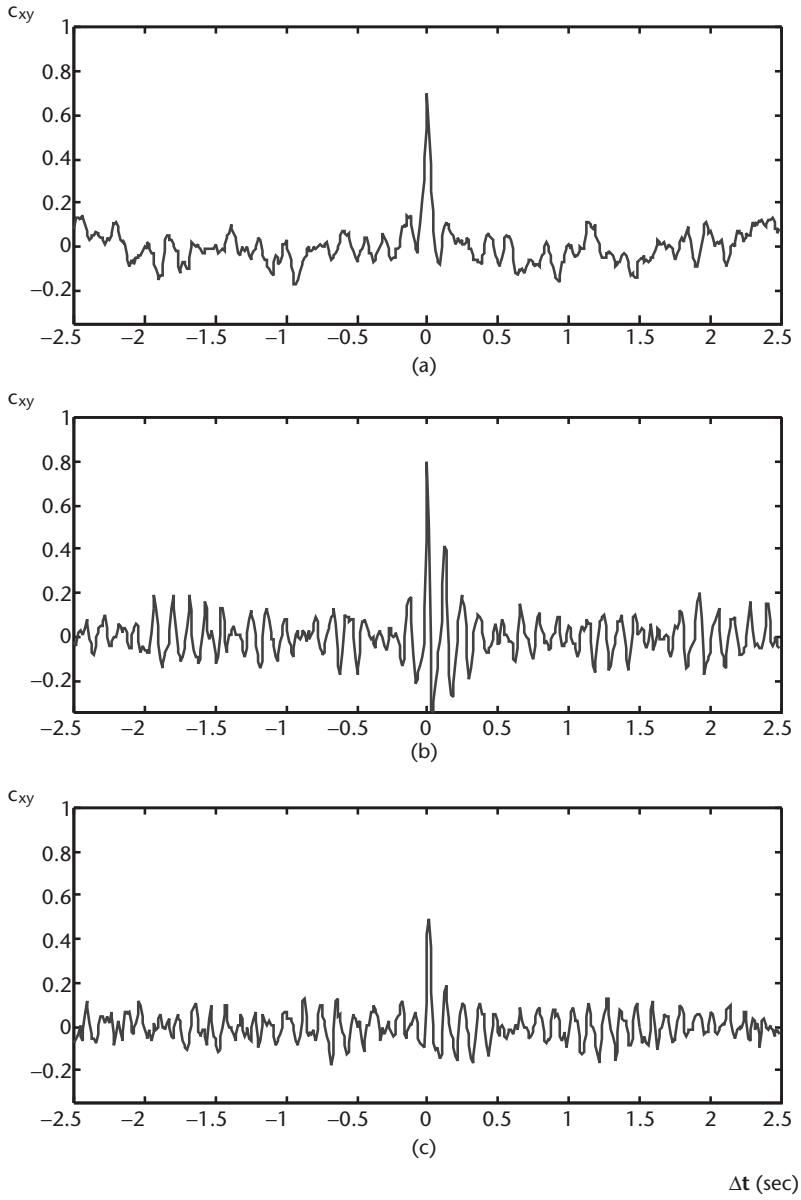

Figure 4.2 (a–c) Cross-correlation values for the three signals of Figure 4.1 as a function of the time delay τ between both signals.

$$\Gamma_{xy}(\omega) = \frac{\left|\left\langle C_{xy}(\omega)\right\rangle\right|}{\sqrt{\left\langle C_{xx}(\omega)\right\rangle}\sqrt{\left\langle C_{xx}(\omega)\right\rangle}} \tag{4.3}$$

is named the coherence function. As mentioned earlier, this measure is particularly useful when synchronization is limited to some particular EEG frequency band (for a review, see [12]). Note that without the segmentation of the data introduced to

Table 4.1 Cross-Correlation, Coherence, and Phase Synchronization Values for the Three Examples of Figure 4.1

Example	c_{xy}	Γ_{xy}	γ
A	0.70	0.88	0.59
B	0.79	0.86	0.71
C	0.42	0.40	0.48

estimate each auto spectrum and cross spectrum, the coherence function of (4.3) gives always a trivial value of 1.

Figure 4.3 shows the power spectra and coherence values for the three examples of Figure 4.1. For the spectral estimates we used half-overlapping segments of 128 data points tapered with a Hamming window in order to diminish border effects [11]. In the case of example A, the spectrum resembles a power-law distribution with the main activity concentrated between 1 and 10 Hz. This range of frequencies has the largest coherence values. For examples B and C, a more localized spectral distribution is seen, with a peak around 7 to 10 Hz and a harmonic around 15 Hz. These peaks correspond to the frequency of the spikes of Figure 4.1.

It is already clear from the spectral distribution that there is a better matching between the power spectra of the right and left channels of example B than for example C. This is reflected in the larger coherence values of example B, with a significant synchronization for this frequency range. In contrast, coherence values are much lower for example C, seeming significant only for the low frequencies (below 6 Hz). In Table 4.1 the coherence values at a frequency of 9 Hz—the main frequency of the spikes of examples B and C—are reported. As was the case for the cross correlation, note that the coherence function does not distinguish well between examples A and B. From Figure 4.3, there is mainly a difference for frequencies larger than about 11 Hz, but this just reflects the lack of activity at this frequency range for example A, whereas in example B it reflects the synchronization between the high-frequency harmonics of the spikes. Even then, it is difficult to assess which frequency should be taken to rank the overall synchronization of the three signals (but some defenders of coherence may still argue that an overall synchronization value is meaningless).

4.3 Mutual Information Analysis

The cross-correlation and coherence functions evaluate linear relationships between two signals in the time and frequency domains, respectively. These measures are relatively simple to compute and interpret but have the main disadvantage of being linear and, therefore, not sensitive to nonlinear interactions. In this section we describe a measure that is sensitive to nonlinear interactions, but with the caveat that it is usually more difficult to compute, especially for short datasets.

Suppose we have a discrete random variable X with M possible outcomes $X_1, \ldots, X_M$, which can, for example, be obtained by partitioning of the X variables into M bins. Each outcome has a probability p_i, $i = 1, \ldots, M$, with $p_i = 0$ and $\Sigma p_i = 1$. A first estimate of these probabilities is to consider $p_i = n_i/N$, where n_i is the probability of

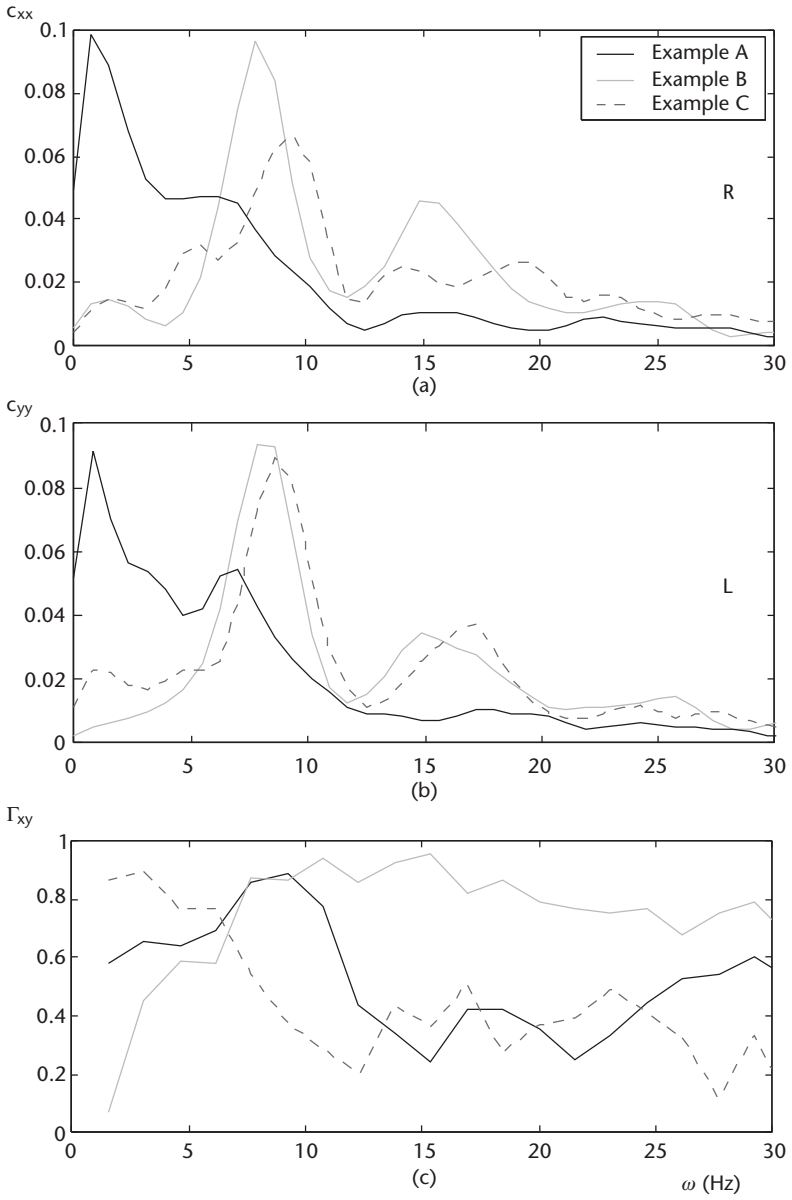

Figure 4.3 (a–c) Power spectral estimation for the three signals of Figure 4.1 and the corresponding coherence estimation as a function of frequency.

occurrence of X_i after N samples. Note, however, that for a small number of samples this naïve estimate may not be appropriate and it may be necessary to introduce corrections terms [8]. Given this set of probabilities, we can define the Shannon entropy as follows:

$$I(X) = -\sum_{i=1}^{M} p_i \log p_i \tag{4.4}$$

The Shannon entropy is always positive and it measures the information content of X, in bits, if the logarithm is taken with base 2.

Next, suppose we have a second discrete random variable Y and that we want to measure its degree of synchronization with X. We can define the joint entropy as

$$I(X,Y) = -\sum_{i,j} p_{ij}^{XY} \log p_{ij}^{XY} \tag{4.5}$$

in which p_{ij}^{XY} is the joint probability of obtaining an outcome $X = X_i$ and $Y = Y_i$. For independent systems, one has $p_{ij}^{XY} = p_i^X p_j^Y$ and therefore, $I(X,Y) = I(X) + I(Y)$. Then, the mutual information between X and Y is defined as

$$MI(X,Y) = I(X) + I(Y) - I(X,Y) \tag{4.6}$$

The mutual information gives the amount of information of X one obtains knowing Y and vice versa. For independent signals, $MI(X,Y) = 0$; otherwise, it takes positive values with a maximum of $MI(X,Y) = I(X) = I(Y)$ for identical signals.

Alternatively, the mutual information can be seen as a Kullback-Leibler entropy, which is an entropy measure of the similarity of two distributions [13, 14]. Indeed, (4.6) can be written in the form

$$MI(X,Y) = \sum p_{ij}^{XY} \log \frac{p_{ij}^{XY}}{p_i^X p_j^Y} \tag{4.7}$$

Then, considering a probability distribution $q_{ij}^{XY} = q_i^X q_j^Y$, (4.7) is a Kullback-Leibler entropy that measures the difference between the probability distributions p_{ij}^{XY} and q_{ij}^{XY}. Note that q_{ij}^{XY} is the correct probability distribution if the systems are independent and, consequently, the mutual information measures how different the true probability distribution p_{ij}^{XY} is from another one in which independence between X and Y is assumed.

Note that it is not always straightforward to estimate MI from real recordings, especially since an accurate estimation requires a large number of samples and small partition bins (a large M). For the joint probability densities p_{ij}^{XY} in particular, there will usually be a large number of bins that will not be filled by the data, which may produce an underestimation of the value of MI. Several different proposals have been made to overcome these estimation biases whose description is outside the scope of this chapter. For a recent review, the reader is referred to [15]. In the particular case of the examples of Figure 4.1, the estimation of mutual information depended largely on the partition of the stimulus space used [8].

4.4 Phase Synchronization

All of the previous measures we described are sensitive to relationships both in the amplitudes and phases of the signals. Interestingly, in some cases the phases of the signals may be related but the amplitudes may not. Phase synchronization measures are particularly suited for these cases because they measure any phase relationship between signals independent of their amplitudes. The basic idea is to generate an

analytic signal from which a phase and a phase difference between two signals can be defined.

Suppose we have a continuous signal $x(t)$, from which we can define an analytic signal

$$Z_x(t) = x(t) + j\tilde{x}(t) = A_x(t)e^{j\phi_x(t)} \tag{4.8}$$

where $\tilde{x}(t)$ is the Hilbert transform of $x(t)$:

$$\tilde{x}(t) \equiv (Hx)(t) = \frac{1}{\pi} P.V. \int_{-\infty}^{+\infty} \frac{x(t')}{t - t'} dt' \tag{4.9}$$

where P.V. refers to the Cauchy principal value. Similarly, we can define A_y and ϕ_y from a second signal $y(t)$. Then, we define the (n,m) phase difference of the analytic signals as

$$\phi_{xy}(t) \equiv n\phi_x(t) - m\phi_y(t) \tag{4.10}$$

with n, m integers. We say that x and y are m:n synchronized if the (n,m) phase difference of their analytic signals of (4.10) remains bounded for all t. In most cases, only the (1:1) phase synchronization is considered. The phase synchronization index is defined as follows [16–18]:

$$\gamma \equiv \left| \left\langle e^{j\phi_{xy}(t)} \right\rangle_t \right| = \sqrt{\left\langle \cos\phi_{xy}(t) \right\rangle_t^2 + \left\langle \sin\phi_{xy}(t) \right\rangle_t^2} \tag{4.11}$$

where the angle brackets denote average over time. The phase synchronization index will be zero if the phases are not synchronized and will be one for a constant phase difference. Note that for perfect phase synchronization the phase difference is not necessarily zero, because one of the signals could be leading or lagging in phase with respect to the other. Alternatively, a phase synchronization measure can be defined from the Shannon entropy of the distribution of phase differences $\phi_{xy}(t)$ or from the conditional probabilities of $\phi_x(t)$ and $\phi_y(t)$ [19].

An interesting feature of the phase synchronization is that it is parameter free. However, it relies on an accurate estimation of the phase. In particular, to avoid misleading results, broadband signals (as is usually the case of EEGs) should be first bandpass filtered in the frequency band of interest before calculating phase synchronization.

It is also possible to define a phase synchronization index from the wavelet transform of the signals [20]. In this case the phases are calculated by convolving each signal with a Morlet wavelet function. The main difference with the estimation using the Hilbert transform is that a central frequency ω_0 and a width of the wavelet function should be chosen and, consequently, this measure is sensitive to phase synchronization in a particular frequency band. It is of particular interest to mention that both approaches—either defining the phases with the Hilbert or with the wavelet transform—are intrinsically related (for details, see [8]).

Figure 4.4 shows the time evolution of the (1:1) phase differences $\phi_{xy}(t)$ estimated using (4.10) for the three examples of Figure 4.1. It is clear that the phase differences of example B are much more stable than the one of the other two examples. The values of phase synchronization for the three examples are shown in Table 4.1 and are in agreement with the general tendency found with the other measures; that is, $\text{Sync}_B > \text{Sync}_A > \text{Sync}_C$. Because by using the Hilbert transform (the same applies to the wavelet transform) we can extract an instantaneous phase for each signal, we can see how phase synchronization varies with time, as shown in the bottom panel

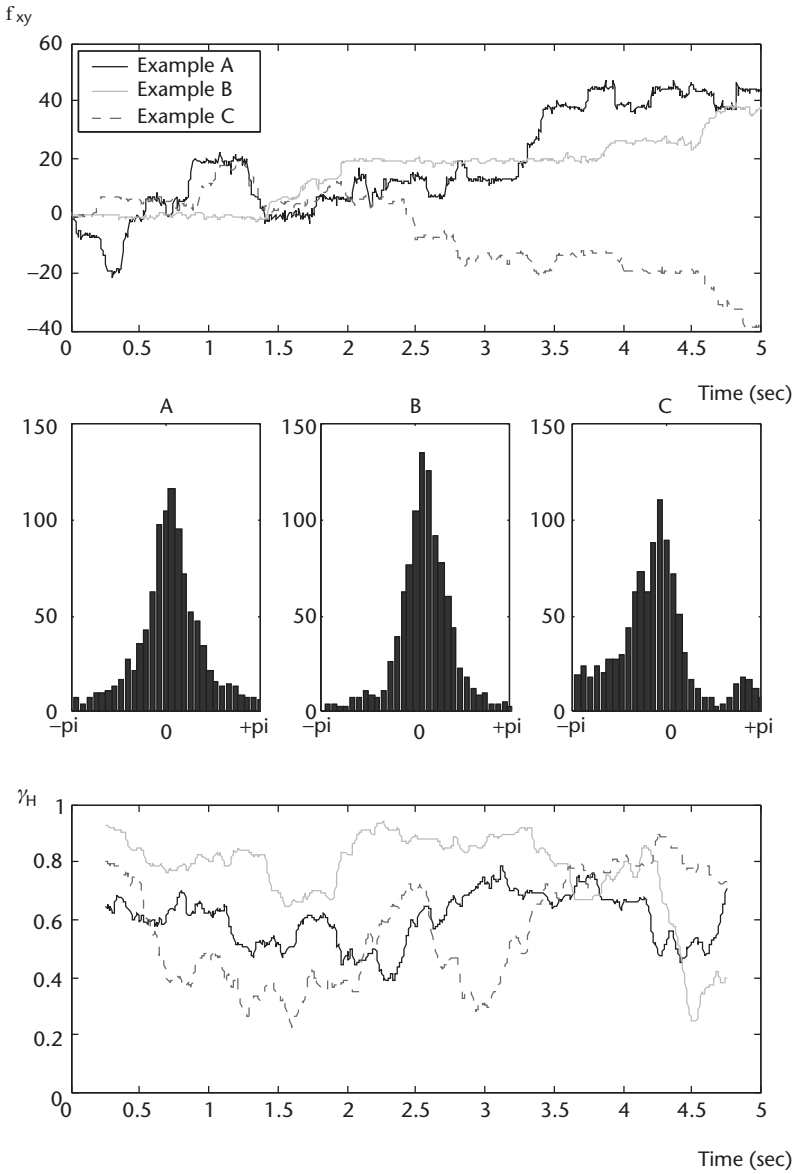

Figure 4.4 (Top) (1:1) phase difference for the three examples of Figure 4.1. (Middle) Corresponding distribution of the phase differences. (Bottom) Time evolution of the phase synchronization index.

of Figure 4.4. Note the variable degree of synchronization, especially for example C, which has a large increase of synchronization after second 3.

4.5 Conclusion

In this chapter we applied several linear and nonlinear measures of synchronization to three typical EEG signals. The first measure we described was the cross-correlation function, which is so far the most often used measure of correlation in neuroscience. We then described how to estimate coherence, which gives an estimation of the linear correlation as a function of the frequency. In comparison to cross correlation, the advantage of coherence is that it is sensitive to correlations in a limited frequency range. The main limitation of cross correlation and coherence is that they are linear measures and are therefore not sensitive to nonlinear interactions.

Using the information theory framework, we showed how it is possible to have a nonlinear measure of synchronization by estimating the mutual information between two signals. However, the main disadvantage of mutual information is that it is more difficult to compute, especially with short datasets. Finally, we described phase synchronization measures to quantify the interdependences of the phases between two signals, irrespective of their amplitudes. The phases can be computed using either the Hilbert or the wavelet transform, with similar results.

In spite of the different definitions and sensitivities of different characteristics of the signals, we saw that all of these measures gave convergent results and that naïve estimations based on visual inspection can be very misleading. It is not possible in general to assert which is the best synchronization measure. For example, for very short datasets mutual information may be not reliable, but it could be very powerful if long datasets are available. Coherence may be very useful for studying interactions at particular frequency bands, and phase synchronization may be the measure of choice if one wants to focus on phase relationships. In summary, the "best measure" depends on the particular data and questions at hand.

References

[1] Strogatz, S., *Sync: The Emerging Science of Spontaneous Order,* New York: Hyperion Press, 2003.

[2] Niedermeyer, E., "Epileptic Seizure Disorders," in *Electroencephalography: Basic Principles, Clinical Applications, and Related Fields,* 3rd ed., E. Niedermeyer and F. Lopes Da Silva, (eds.), Baltimore, MD: Lippincott Williams & Wilkins, 1993.

[3] Engel, A. K., and W. Singer, "Temporal Binding and the Neural Correlates of Sensory Awareness," *Trends Cogn. Sci.,* Vol. 5, No. 1, 2001, pp. 16–25.

[4] Singer, W., and C. M. Gray, "Visual Feature Integration and the Temporal Correlation Hypothesis," *Ann. Rev. Neurosci.,* Vol. 18, 1995, pp. 555–586.

[5] Rieke, F., et al., *Spikes: Exploring the Neural Code*, Cambridge, MA: MIT Press, 1997.

[6] Varela, F., et al., "The Brainweb: Phase Synchronization and Large-Scale Integration," *Nature Rev. Neurosci.,* Vol. 2, No. 4, 2001, pp. 229–239.

[7] van Luijtelaar, G., and A. Coenen, *The WAG/Rij Rat Model of Absence Epilepsy: Ten Years of Research,* Nyonegen: Nijmegen University Press, 1997.

[8] Quian Quiroga, R., et al., "Performance of Different Synchronization Measures in Real Data: A Case Study on Electroencephalographic Signals," *Phys. Rev. E,* Vol. 65, No. 4, 2002, 041903.

[9] Pereda, E., R. Quian Quiroga, and J. Bhattacharya, "Nonlinear Multivariate Analysis of Neurophysiological Signals," *Prog. Neurobiol.,* Vol. 77, No. 1–2, 2005, pp. 1–37.

[10] Quian Quiroga, R., J. Arnhold, and P. Grassberger, "Learning Driver-Response Relationships from Synchronization Patterns," *Phys. Rev. E,* Vol. 61, No. 5, Pt. A, 2000, pp. 5142–5148.

[11] Oppenheim, A. V., and R. W. Schafer, *Discrete-Time Signal Processing*, Upper Saddle River, NJ: Prentice-Hall, 1999.

[12] Lopes da Silva, F., "EEG Analysis: Theory and Practice," in *Electroencephalography: Basic Principles, Clinical Applications and Related Fields,* E. Niedermeyer and F. Lopes da Silva, (eds.), Baltimore, MD: Lippincott Williams & Wilkins, 1993.

[13] Quian Quiroga, R., et al., "Kullback-Leibler and Renormalized Entropies: Applications to Electroencephalograms of Epilepsy Patients," *Phys. Rev. E,* Vol. 62, No. 6, 2000, pp. 8380–8386.

[14] Cover, T. M., and J. A. Thomas, *Elements of Information Theory*, New York: Wiley, 1991.

[15] Panzeri, S., et al., "Correcting for the Sampling Bias Problem in Spike Train Information Measures," *J. Neurophysiol.,* Vol. 98, No. 3, 2007, pp. 1064–1072.

[16] Mormann, F., et al., "Mean phase Coherence as a Measure for Phase Synchronization and Its Application to the EEG of Epilepsy Patients," *Physica D,* Vol. 144, No. 3–4, 2000, pp. 358–369.

[17] Rosenblum, M. G., et al., "Phase Synchronization: From Theory to Data Analysis," in *Neuroinformatics: Handbook of Biological Physics,* Vol. 4, F. Moss and S. Gielen, (eds.), New York: Elsevier, 2000.

[18] Rosenblum, M. G., A. S. Pikovsky, and J. Kurths, "Phase Synchronization of Chaotic Oscillators," *Phys. Rev. Lett.,* Vol. 76, No. 11, 1996, p. 1804.

[19] Tass, P., et al., "Detection of n:m Phase Locking From Noisy Data: Application to Magnetoencephalography," *Phys. Rev. Lett.,* Vol. 81, No. 15, 1998, p. 3291.

[20] Lachaux, J. P., et al., "Measuring Phase Synchrony in Brain Signals," *Human Brain Mapping,* Vol. 8, No. 4, 1999, pp. 194–208.